Review

# Performance of anode-supported solid oxide fuel cell using novel ceria electrolyte

Jin Soo Ahn, Shobit Omar [1], Heesung Yoon, Juan C. Nino, Eric D. Wachsman *

Florida Institute for Sustainable Energy, University of Florida, 207 MAE, Gainesville, FL 32611, USA

## ARTICLE INFO

## ABSTRACT

The potential of a novel co-doped ceria material $Sm_{0.075}Nd_{0.075}Ce_{0.85}O_{2-\delta}$ as an electrolyte was investigated under fuel cell operating conditions. Conventional colloidal processing was used to deposit a dense layer of $Sm_{0.075}Nd_{0.075}Ce_{0.85}O_{2-\delta}$ (thickness 10 μm) over a porous Ni-gadolinia doped ceria anode. The current–voltage performance of the cell was measured at intermediate temperatures with 90 cm$^3$ min$^{-1}$ of air and wet hydrogen flowing on cathode and anode sides, respectively. At 650 °C, the maximum power density of the cell reached an exceptionally high value of 1.43 W cm$^{-2}$, with an area specific resistance of 0.105 Ω cm$^2$. Impedance measurements show that the power density decrease with decrease in temperature is mainly due to the increase in electrode resistance. The results confirm that $Sm_{0.075}Nd_{0.075}Ce_{0.85}O_{2-\delta}$ is a promising alternative electrolyte for intermediate temperature solid oxide fuel cells.

© 2009 Elsevier B.V. All rights reserved.

## Contents

## 1. Introduction

Due to their potential high efficiency, solid oxide fuel cells (SOFCs) not only conserve valuable natural resources but also assist in reducing pollution and greenhouse gas emissions. However, long-term degradation problems associated with the high-temperature operation, and relatively expensive manufacturing costs remain the main challenges for the commercialization of this technology [1]. Lowering the operating temperature to an intermediate temperature (IT) range (400–700 °C), not only

improves reliability, but also lowers the cost, and time and energy it takes to heat up to the operating temperature. This will extend its application domain to residential power and portable devices. However, with the current state-of-the-art SOFC materials, it is not possible to obtain sufficient power in the IT range. This is because of high ohmic losses and electrode polarization, which have a detrimental effect on performance and efficiency. Thus, there is a need to develop materials that show improved properties in the IT range.

High ionic conductivity solid oxide electrolytes are critical for the development of SOFCs that can successfully generate reasonable power at IT range [2]. In recent years, doped ceria electrolytes have emerged as a potential candidate due to their higher ionic conductivity than that of yttria stabilized zirconia (YSZ) at intermediate temperatures [1,3]. Among doped ceria materials, $Gd_{0.10}Ce_{0.90}O_{2-\delta}$ (GDC) was widely accepted to exhibit the highest ionic conductivity [4]. However, our previous results have shown that co-doping based on $Sm^{3+}$ and $Nd^{3+}$ leads to further enhancement in the

* Corresponding author at: University of Maryland Energy Research Center, University of Maryland, College Park, MD 20742-2115. Tel.: +1 301 405 8193; fax: +1 301 314 8514.
    E-mail address: ewach@umd.edu (E.D. Wachsman).
[1] Current address: Risø National Laboratory for Sustainable Energy, Fuel Cells and Solid State Chemistry Division, Technical University of Denmark, DK-4000 Roskilde, Denmark.

ionic conductivity in ceria systems [3]. Optimization of dopant concentration in the $Sm_{x/2}Nd_{x/2}Ce_{1-x}O_{2-\delta}$ system resulted in the development of $Sm_{0.075}Nd_{0.075}Ce_{0.85}O_{2-\delta}$ (SNDC), which exhibits 30% higher grain ionic conductivity than that of GDC at 550 °C in air.

In the present work, the potential of SNDC as an alternative electrolyte is further investigated by testing the performance in a SOFC. An anode-supported SOFC is fabricated, with SNDC as the electrolyte. A novel anode functional layer (AFL) with precursor solution was employed to provide a better surface for colloidal deposition of the SNDC electrolyte [5,6]. The performance of the SOFC at intermediate temperatures is discussed in this work.

## 2. Experimental

The Ni–GDC anode supports were synthesized by tape casting a mixture of NiO (Alfa Aesar, 99% purity, CAS 1313) and GDC (Rhodia, LOT H-050708) powders. The powder mixture contains 65 wt.% of NiO. Both raw oxide powders were weighed (to obtain 150 g batch of powder mixture), and were mixed in toluene (Fisher Scientific) (13.6 wt.%) and ethanol (Fisher Scientific) (11.3 wt.%). A 1 wt.% of solsperse (Air Products and Chemicals) was added to the slurry as dispersant. Further, a mixture of di-n butyl phthalate (Alfa Aesar) (4.3 wt.%), and polyethylene glycol (Fisher Scientific) (0.8 wt.%) was added as plasticizer, while polyvinyl butyral (Acros Organics) (8.4 wt.%) was added to the slurry as binder. Mixing was performed using ball milling for 24 h. The resulting slurry was then transferred to a vacuum chamber, for de-airing. During this process, the slurry was constantly magnetically stirred to avoid any solidification. The slurry was then tape-cast using a tape-caster (Procast from DHI, Inc.) with a caster speed of 10 cm min$^{-1}$. The substrate temperature was maintained at 80 °C during this process. The NiO–GDC tape (thickness ~800 μm) was subsequently dried at 100 °C for 2 h. Circular green tapes with 32 mm diameter were then punched out from the tape, and partially sintered at 900 °C for 2 h. The anode supports were then coated with GDC precursor solutions as an AFL (equivalent to 1.5 mg of GDC per cm$^2$) by spray coating. Details of the AFL deposition and its impact on the performance of SOFCs are described elsewhere [6].

The co-precipitation technique was used to synthesize phase pure powder of SNDC. Highly pure cerium nitrate ($Ce(NO_3)_3 \cdot 6H_2O$, Alfa Aesar, 99.99%), samarium nitrate ($Sm(NO_3)_3 \cdot 6H_2O$, Aldrich, 99.999%), and neodymium nitrate ($Nd(NO_3)_3 \cdot 6H_2O$, Alfa Aesar, 99.9%) were used as starting materials. They were weighed in stoichiometric proportions and dissolved in de-ionized water to produce an aqueous solution. Excess ammonia solution (Acros Organics, 28–30% of $NH_3$ solution in water) was added to the stirred solution to increase the pH value to 12. The addition of ammonia solution resulted in the formation of yellowish brown color precipitate. The precipitate was washed and filtered, and then subsequently dried at 80 °C for 12 h. The agglomerated powder was ground to fine particles using a mortar and pestle. The powder was then calcined at 900 °C for 10 h in air. After calcination, the agglomerated powder was ground again using a mortar and pestle to fine size particles which were then sieved (212 μm aperture opening).

An X-ray diffractometer (XRD) with Cu Kα tube source and curved position sensitive detector (CPS120 INEL Inc.) was used to obtain the XRD pattern of the SNDC powder. A monochromator crystal was used to separate out Cu $K_{\alpha2}$ from the incident X-ray beam, providing a monochromatic Cu $K_{\alpha1}$ incident beam. Peak positions in the XRD pattern were determined by fitting each individual peak with symmetric Pearson VII profiles using commercially available software (i.e., Solver add-in for Microsoft Excel).

For the deposition of the electrolyte on the anode support (GDC AFL/NiO-GDC anode), the SNDC powder was ball-milled for 24 h, in ethanol medium with solsperse as a dispersing agent. For a typi-

cal 10 g batch of SNDC powder, 26.3 wt.% of ethanol and 1 wt.% of solsperse were used. After 24 h of ball milling, 10 wt.% of polyvinyl butyral and di-n butyl phthalate (3 wt.%) were added to the slurry. The ceramic slurry was again ball-milled for another 24 h. Before deposition the ceramic slurry was placed in an ultrasonic water bath for 10 min. The ceramic slurry of SNDC was then dip-coated twice onto the anode surface. After each deposition, the sample was dried at room temperature for 30 min. The electrolyte deposited samples were subsequently heat-treated at 120 °C for 5 h. The bi-layered structure of the electrolyte and anode was then co-sintered at 1550 °C for 4 h using a 3 °C min$^{-1}$ ramp rate in air.

The cathode ink was prepared by mixing $La_{0.6}Sr_{0.4}Co_{0.2}Fe_{0.8}O_{3-\delta}$ (Praxair Specialty Ceramics, 99.9% purity) and the GDC powder in a 1:1 weight ratio, using mortar and pestle. Alpha-terpiniol (40 wt.% of the powder) was added as a solvent, and di-n butyl phthalate (6.7 wt.% of the powder) was used as a plasticizer. Further, polyvinyl butyral (2.3 wt.% of the powder) dissolved in ethanol (21 wt.% of the powder) was added as a binder. After mixing and grinding the cathode ink in mortar and pestle for 1 h, the ink was brush-painted evenly onto the SNDC electrolyte (deposited on NiO/GDC tape). The first layer of cathode ink was dried in an oven at 120 °C for 1 h. A second layer of the same cathode ink was then evenly brush-painted on top of the first layer. The samples were then fired at 1100 °C for 1 h. Pt paste (CL11-5349, Heraeus) was brush-painted on both electrodes and used to attach Pt mesh and Au connecting wires as a current collector. The samples were then heat-treated at 900 °C for 1 h.

The fuel cell samples were sealed (anode side) to a zirconia tube in a custom-made testing apparatus using two-part ceramabond sealant (a mixture of 517-powder and 517-liquid from Aremco). The setup was then placed into a furnace, cured, and taken up to testing temperature. Dry air and $H_2/H_2O$ (3 vol% $H_2O$) gas mixtures were used as the oxidant and fuel gases, respectively. The 90 cm$^3$ min$^{-1}$ of dry air and wet hydrogen were supplied to the cathode and anode side, respectively. The cell open circuit potential (OCP) was monitored using a Solartron 1287 potentiostat until a stable value was reached, and the current–voltage (I–V) measurements were taken with the same instrument. The impedance measurements were carried out at open circuit conditions using two-point probe ac impedance spectroscopy technique. A PARSTAT 2273 (Princeton Applied Research) frequency response analyzer was used for impedance measurement. Impedance spectra were measured from 10 kHz to 0.01 Hz with ac signal strength of 10 mV, at various temperatures from 500 to 650 °C.

A JEOL 6400 V scanning electron microscope (SEM) was used to characterize the microstructure of the fuel cell sample with an accelerating voltage of 15 kV.

## 3. Results and discussion

### 3.1. XRD

Fig. 1 shows the XRD profile of the calcined powder of SNDC taken at room temperature. The powder is phase pure with cubic fluorite structure. The best estimate of the lattice constant ($a_o$) was calculated using the least-squares extrapolation method [7]. The lattice parameter of SNDC synthesized using co-precipitation technique was $5.4340 \pm 0.0017$ Å. The estimated lattice parameter value is close to the value (5.4351 Å) obtained from the lattice parameter ($a$) and dopant concentration ($x$) relationship for $Sm_{x/2}Nd_{x/2}Ce_{1-x}O_{2-\delta}$ reported in our previous publication [4].

### 3.2. Particle size

Fig. 2 shows the particle size distribution of the SNDC and the commercially obtained $La_{0.6}Sr_{0.4}Co_{0.2}Fe_{0.8}O_{3-\delta}$ (LSCF) pow-

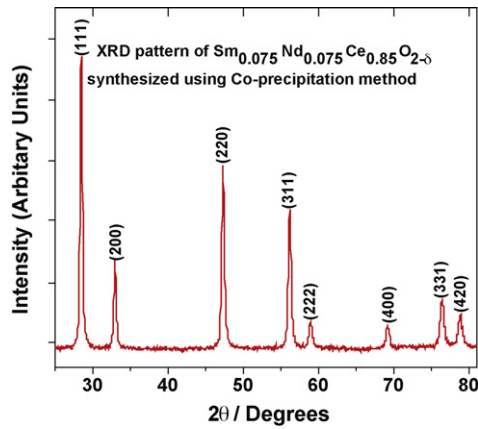**Fig. 1.** XRD pattern of $Sm_{0.075}Nd_{0.075}Ce_{0.85}O_{2-\delta}$ synthesized using co-precipitation technique.

ders. The particle size distribution of the phase pure SNDC powder synthesized using co-precipitation technique was measured using a Beckman Coulter LS13320 particle size analyzer. The particle size distribution of the LSCF powder was provided by the Praxair Specialty Ceramics. The SNDC particles were less than 1 μm in diameter, with a mean particle size of 0.095 μm and a monodisperse particle size distribution.

The GDC powder obtained from Rhodia was comprised of very fine particles of size less than 100 nm [5]. On the other hand, the NiO particles were mostly micron-sized [5]. Large particles of NiO, after reduction in $H_2$, resulted in the anode porosity. The LSCF powder used for the cathode exhibited a bi-modal particle size distribution, with most of the particles around 1 μm in size (Fig. 2).

### 3.3. Microstructural analysis

Fig. 3 shows the microstructure of the SNDC surface (a), and the cross-section of the fuel cell sample (b). It can be seen both in the cross-sectional and surface micrographs that the electrolyte is densely sintered except for a few isolated residual pores. From the SEM image, while irregular, the thickness of the SNDC electrolyte is estimated to be ∼10 μm. This suggests that the SNDC electrolyte can be easily deposited with ceramic processes such as colloidal deposition.

Further, the nickel (reduced form of NiO) particles in the anode are large compared to LSCF particles in the cathode. This is mainly due to the large particle size of the NiO starting powder. Although, hydrogen oxidation in the anode is kinetically more favorable than
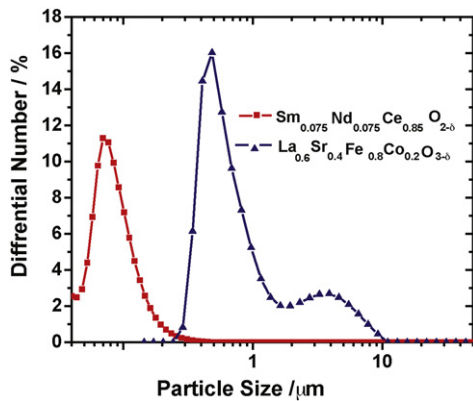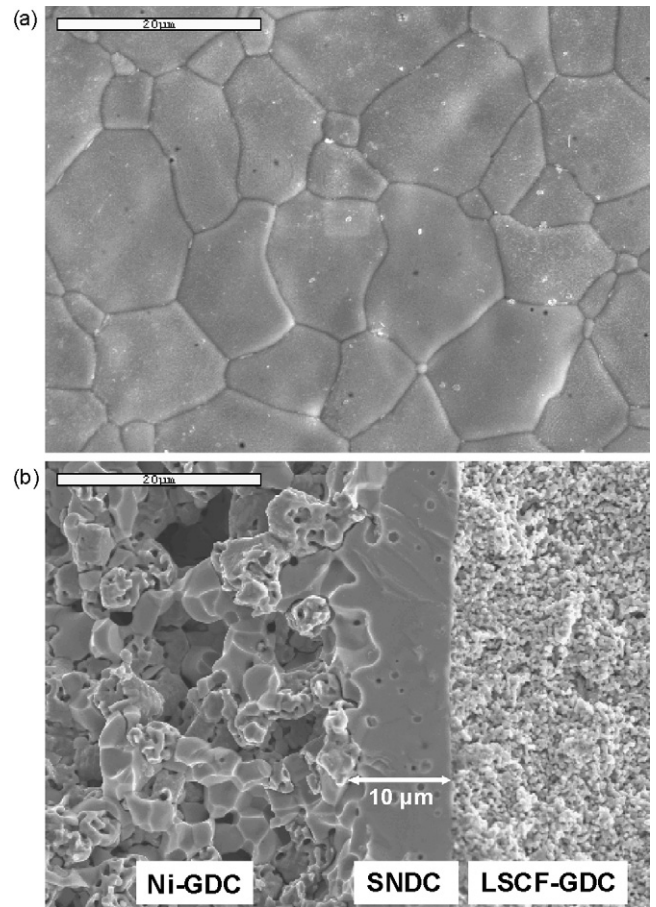


**Fig. 3.** FE-SEM images of (a) surface of the electrolyte, and (b) cross-section view of electrodes and electrolyte.

oxygen reduction in the cathode, significantly large Ni particle size near the electrolyte/anode interface can cause high anodic activation polarization at low temperatures. In our previous work, it was shown that anode polarization can be significantly reduced by using an AFL between anode and electrolyte layers [5,6]. In the present work, the AFL was employed to reduce the additional anode polar-
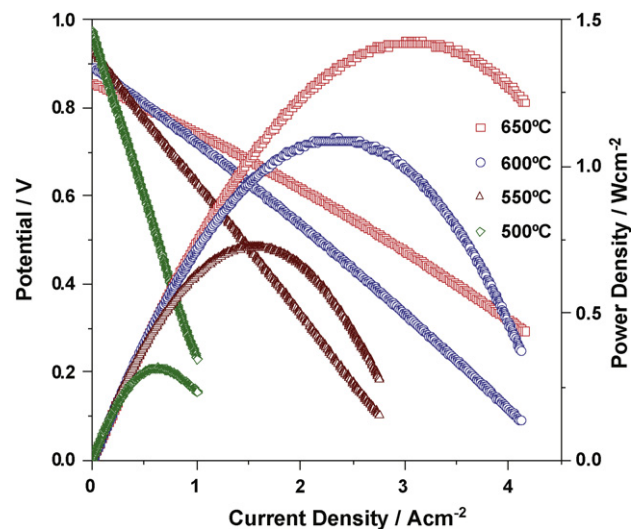


**Fig. 2.** Particle size distribution of $Sm_{0.075}Nd_{0.075}Ce_{0.85}O_{2-\delta}$ synthesized using co-precipitation technique and $La_{0.6}Sr_{0.4}Co_{0.2}Fe_{0.8}O_{3-\delta}$ (obtained from Praxair Specialty Ceramics).



**Fig. 4.** The *I–V* characteristics and the power densities of the SOFC sample with $Sm_{0.075}Nd_{0.075}Ce_{0.85}O_{2-\delta}$ electrolyte at various temperatures ranging from 500 to 650 °C in 90 cm³ min⁻¹ of both dry air and wet hydrogen.
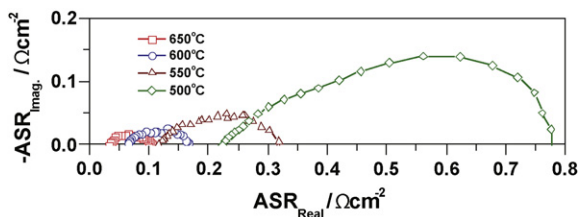
**Fig. 5.** Impedance spectrum of the SOFC cell measured at different temperatures.

**Table 1**
Comparison between the total ASR obtained from *I–V* characteristic and impedance measurement. The ohmic contribution towards the total ASR is also shown.

| Temperature (°C) | Total ASR$_{I–V}$ ($\Omega\,cm^2$) | Total ASR$_{Impe.}$ ($\Omega\,cm^2$) | ASR$_{Electrode}$ ($\Omega\,cm^2$) | ASR$_{Ohmic}$ ($\Omega\,cm^2$) |
|---|---|---|---|---|
| 650 | 0.106 | 0.105 | 0.072 | 0.033 |
| 600 | 0.166 | 0.167 | 0.103 | 0.064 |
| 550 | 0.323 | 0.318 | 0.201 | 0.117 |
| 500 | 0.783 | 0.776 | 0.552 | 0.224 |

ization caused by the use of large NiO powder. Details on the change in the surface microstructure for the same anode support using the AFL can be found elsewhere [6].

### 3.4. Power density

Fig. 4 shows the *I–V* characteristics of the SOFC with SNDC as an electrolyte at temperatures ranging from 500 to 650 °C. The OCP values obtained were 0.86, 0.89, 0.93 and 0.96 V at 650, 600, 550 and 500 °C, respectively. The obtained OCP values were higher than previous typical OCP values achieved with GDC as an electrolyte, using similar fabrication route and experimental setup (e.g., 0.80 V at 650 °C) [5,6].

Fig. 4 also shows the power density as a function of current density. The maximum power densities achieved in the test cell were 1.43, 1.10, 0.73 and 0.32 W cm$^{-2}$ at 650, 600, 550, and 500 °C, respectively. For the intermediate temperatures, the obtained power densities were exceptionally high and higher than those obtained from similarly prepared SOFC samples with 10 μm thick GDC electrolyte (1 W cm$^{-2}$ at 650 °C) [5,6]. This could be due in part to the high ionic conductivity of SNDC electrolyte. However, it is important to note that the *I–V* characteristics and the maximum power density of the SOFC is a function of numerous processing and material variables. For this reason, the performance of SNDC electrolyte cannot be directly compared with that of GDC using *I–V* characteristics. Comparison between the ionic conductivity of SNDC and GDC electrolytes is reported elsewhere [3,4]. However, the performance testing results suggest that the SNDC electrolyte material can successfully generate high power density in SOFCs operating in the intermediate temperature range.

### 3.5. Impedance analysis

Fig. 5 shows the impedance spectrum of the SOFC at 650, 600, 550 and 500 °C, taken at open circuit conditions. Using impedance
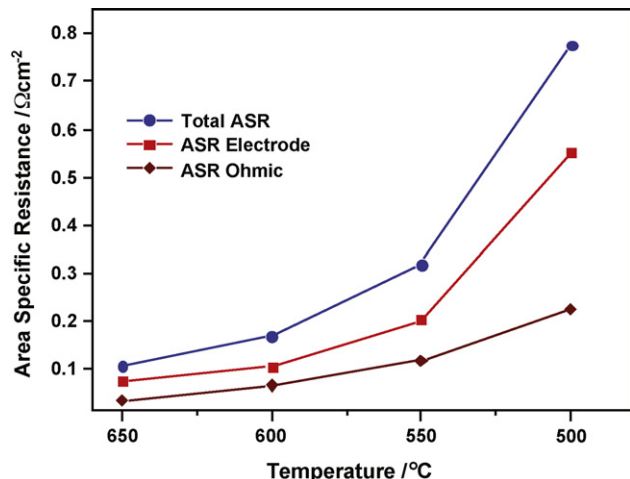
spectroscopy, it is possible to separate out the electrode and ohmic contributions to the total area specific resistance (ASR) value at each temperature. From the high frequency intercept of the impedance spectrum with the real axis, the ohmic ASR value was calculated (after normalizing the resistance to the cathode area of 0.48 cm$^2$). Electrode ASR was determined from the difference between the low and high frequency intercepts (also after normalizing the resistance to the cathode area). Fig. 6 shows the electrode and the ohmic ASR values separated from the total ASR at different temperatures. The rapid increase in the total ASR with decreasing temperature is mainly due to the significant increase in the electrode polarization. This increase in electrode polarization is most likely due to the cathode reaction which is a thermally activated process [8]. In contrast, ohmic ASR values remain relatively small even at lower temperatures.

The total ASR values were also calculated from the gradient of the linearly fitted *I–V* curves. The total ASR values obtained from the impedance measurements and *I–V* characteristics are reported in Table 1. The impedance measurements were done under open circuit conditions, therefore, while fitting the *I–V* curve, the region near zero current (0–0.2 A cm$^{-2}$) was used. Both ASR values from the *I–V* characteristics and the impedance measurement are comparable at all temperatures.

The ohmic and electrode ASR values separated from the total ASR at each temperature are also presented in Table 1. At 650 °C the ohmic contribution to the total ASR is 31%. With decreasing temperature, the ohmic ASR percentage contribution remains comparatively smaller than the electrode ASR. At 500 °C, the relative ohmic contribution to total ASR is reduced to 29%. It is obvious that further improvement in performance can be achieved by reducing the electrode ASR, especially at lower operating temperatures.

Due to the limitations of the two-point impedance technique it is difficult to deconvolute the contribution from each of the electrodes. However, we have demonstrated that the novel AFL between the anode and electrolyte interface reduces the anode polarization by 60% [6]. Due to the temperature dependence of the ASR and the higher activation energy of the oxygen reduction reaction (at the cathode–electrolyte interface), we believe that the increase in total electrode ASR with decreasing temperature is mainly due to the cathode. This indicates that performance can be further enhanced using better cathode materials with higher catalytic activity.

It is also well known that introducing a highly ionic conducting phase in an electrode composite enhances the performance of SOFCs [9]. Since SNDC exhibits higher ionic conductivity than GDC, it is expected that replacing GDC with SNDC in the cathode will further improve SOFC performance and is the subject of future work.

### 4. Conclusion

The performance of SOFCs based on a novel co-doped ceria electrolyte material was tested at intermediate temperatures. Anode-supported SOFCs were fabricated, with SNDC electrolyte deposited on a NiO–GDC composite anode using colloidal pro-



**Fig. 6.** Area specific resistance at different temperatures.

cessing. A $La_{0.6}Sr_{0.4}Co_{0.2}Fe_{0.8}O_{3-\delta}$–GDC composite was used as the cathode. At 650 °C, a maximum power density of 1.43 W cm$^{-2}$ was achieved. The total ASR at 650 °C was only 0.105 $\Omega$ cm$^2$ resulting in this exceptionally high power density.

Impedance analysis revealed that the decrease in power density with decreasing temperature is mainly due to electrode overpotential. The ohmic ASR contribution remained relatively low, only ~30%, down to 500 °C. Therefore, SNDC is a promising electrolyte for intermediate temperature SOFCs.

## Acknowledgements

## References

[1] B.C.H. Steele, Solid State Ionics 129 (2000) 95.
[2] S. Omar, E.D. Wachsman, J.C. Nino, Solid State Ionics 177 (2006) 3199.
[3] S. Omar, E.D. Wachsman, J.C. Nino, Appl. Phys. Lett. 91 (2007) 144106.
[4] S. Omar, E.D. Wachsman, J.C. Nino, Solid State Ionics 178 (2008) 1890.
[5] J.S. Ahn, H.S. Yoon, E.D. Wachsman, ECS Trans. 16 (2008) 335.
[6] J.S. Ahn, H. Yoon, K.T. Lee, M.A. Camaratta, E.D. Wachsman, Fuel Cells (in press), doi:10.1002/fuce.200900005.
[7] A. Pramanick, S. Omar, J.C. Nino, J.L. Jones, J. Appl. Crystallogr. (in press).
[8] M. Godickemeier, K. Sasaki, L.J. Gauckler, I. Riess, Solid State Ionics 86–8 (1996) 691.
[9] E.P. Murray, S.A. Barnett, Solid State Ionics 143 (2001) 265.